Vibrational Dynamics and Heat Capacity of Polychloroprene

Archana Gupta,[1] Parag Agarwal,[1] Neetu Choudhary,[1] Poonam Tandon,[2] V. D. Gupta[2]

[1]*Department of Applied Physics, Institute of Engineering and Technology, M. J. P. Rohilkhand University, Bareilly, India*
[2]*Department of Physics, Lucknow University, Lucknow, India*

Received 5 March 2010; accepted 30 September 2010
DOI 10.1002/app.33488
Published online 17 February 2011 in Wiley Online Library (wileyonlinelibrary.com).

ABSTRACT: Normal modes and their dispersion have been obtained for polychloroprene in the trans form using Wilson's G F matrix method as modified by Higg's for an infinite polymeric chain. Urey Bradley force field has been used. Several new assignments, which are missing in earlier work, are reported. The assignments of lower frequency modes have been confirmed using inelastic neutron scattering data. The characteristic features of dispersion curves have been explained. Variation of heat capacity as a function of temperature has been predicted.
 J Appl Polym Sci 121: 186–195, 2011

Key words: polychloroprene; infrared spectroscopy; phonon dispersion; density of states; heat capacity

INTRODUCTION

Polychloroprene is a widely used polymer and has many industrial applications.[1–4] It is mainly used in rubber industry but it is also important as a raw material for adhesives. Chloroprene rubber has excellent resistance to oil, chemicals, and deterioration, in addition to having flame-retarding properties. It is widely used in automobile parts and in a variety of heavy-duty equipment. Despite its cost, its high durability under harsh conditions makes neoprene rubber a much needed material.

Polychloroprenes have a highly regular structure[5] (Fig. 1) consisting primarily of a linear sequence of the trans-2-chloro-2 butenylene units (—CH_2—CCl=CH—CH_2—), which result from 1,4-addition polymerization of chloroprene. Crystallization studies have shown that small proportions of other structural isomers may also be present.[6,7] A study of infrared absorption spectra of polychloroprene made at different temperatures[5] has shown that the proportion of these structures increases with the increasing polymerization temperature.

Vibrational spectroscopy is an important tool for probing conformation and conformationally sensitive modes of a polymer. The physical properties of a polymer are strongly influenced by the conformation of the polymer. Vibrational spectroscopy, besides providing information about different conformational states, plays an important role in understanding the dynamical behavior of polymer chain. Normal mode analysis helps in precise assignments and identification of spectral features of a molecule of known structure and force field. However, the problem in case of polymers is an order of magnitude more complex than in simple solids mainly because of the absence of simple symmetry and presence of large contents in unit cell. The art of conformational finger printing of molecules by infrared and Raman spectroscopy cannot succeed here. In general, the infrared absorption, Raman spectra, and inelastic neutron scattering from the polymeric systems are very complex and cannot be unraveled without full knowledge of dispersion curves. One cannot appreciate without it, the origin of both, symmetry dependent and independent spectral features. The dispersion curves also facilitate correlation of the microscopic behavior of a crystal with its macroscopic properties such as specific heat, enthalpy, and free energy.

Normal coordinate calculations and assignment of various vibrational modes for trans 1,4 polychloroprene (TPCP) have been reported earlier.[8–11] The agreement between the observed and the calculated frequencies reported by Tabb and Koenig[8] using valence force field is good in the high frequency range (above 900 cm^{-1}) but not so in the lower frequency range. This disagreement has been attributed by the authors themselves to the least reliability of the force constants associated with the chlorine atom

Correspondence to: A. Gupta (drarchana.physics@gmail.com).

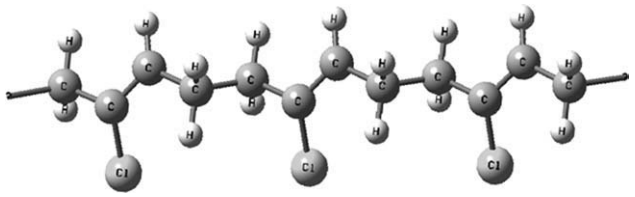

Figure 1 Chain structure of polychloroprene.

that contribute greatest to the spectrum below 900 cm^{-1}. Such studies have also been reported by Petcavich et al.[9] However, they have also used valence force field that does not take into account nonbonded interactions in both gem and tetra positions and tension terms. One of the infirmities of their work is the use of the same force field for both the molecules trans 1,4 polychloroprene and polydichlorobutadiene. The difference between the two is the presence of hydrogen attached to the carbon in one and chlorine in the other. This will cause local perturbations extending at best up to the nearest neighbors. Arjunan et al.[10] have also carried out a normal mode analysis using valence force field. They have not made assignments for the frequencies, characteristics of crystallinity.[11] Further, dispersion of normal modes has not been reported by them. Lack of information on dispersive behavior of normal modes in many polymeric systems has been responsible for incomplete understanding of the polymeric spectra. Thus, a fuller interpretation of IR and Raman spectra demands a re-look at the vibrational dynamics of TPCP. In continuation of our work on the vibrational dynamics of polymeric systems of natural and industrial importance,[12–15] in the present communication we report a complete normal mode analysis using the Urey-Bradley force field (UBFF)[16] as it is more comprehensive than the valence force field. In the UBFF, relatively less parameters are required to express the potential energy and no quadratic cross terms are included in the potential energy expression. The interaction between nonbonded atoms includes these terms and thus the arbitrariness in choosing the force constants is reduced. The normal mode frequencies obtained are in better agreement with the observed IR and Raman data than those reported by previous workers. The calculations lead to some new assignments. In the low frequency region (below 1000 cm^{-1}) the results are compared with the neutron inelastic scattering measurements.[17] We have also reported the predictive values of heat capacity in the range of 10–400 K. To the best of our knowledge, such detailed studies leading to correlation between the microscopic behavior and macroscopic properties of this polymer have not yet been reported.

EXPERIMENTAL DETAILS

Polychloroprene sample was obtained from Sigma Aldrich Chemicals Pvt Ltd, USA.

Fourier transform infrared spectroscopy

The FTIR spectra of polychloroprene were recorded at Bruker IFS 28 spectrometer with a liquid-cooled mercury cadmium telluride (MCT) detector having a resolution of 4 cm^{-1} and 128 scans. The spectra were recorded as thin films cast from carbon disulphide solution onto potassium bromide plates. The observed FTIR spectra are shown in Figure 2(a,b).

Fourier transform Raman spectroscopy

FT Raman spectra of polychloroprene were recorded using an efficient visible micro Raman setup at room temperature. This setup used an excitation laser line of wavelength 514 nm, emitted from an Argon ion laser source with a power of 12 mW to record the vibrational spectra. The scattered Raman light was collected in a back scattering geometry using a microscope objective (ULW 50×). The scattered light was dispersed using a monochromator with 1200 grooves/mm diffraction grating, and an entrance slit width of 200 μm. The Raman signals were detected using liquid nitrogen cooled charged coupled device (CCD) with an optimal sensitivity in the visible range. The total exposure time for each sample was

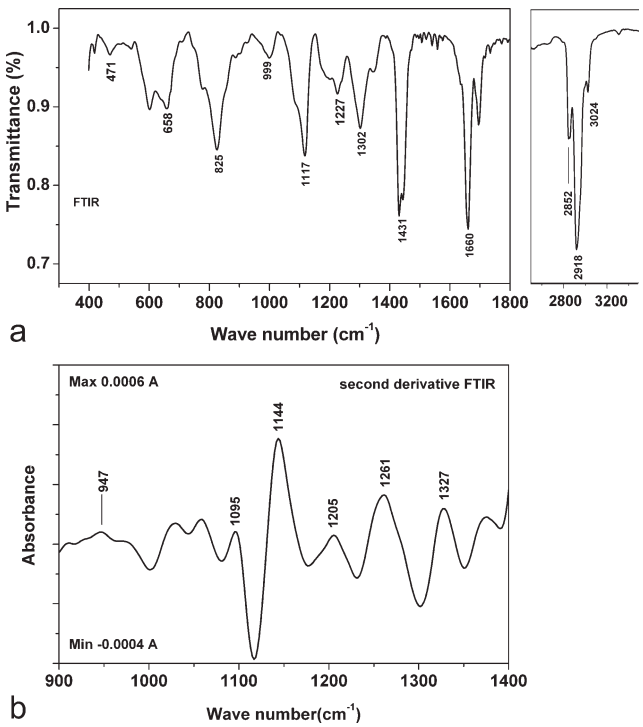

Figure 2 (a) FTIR spectrum of polychloroprene; (b) Second derivative FTIR spectrum of polychloroprene (900–1400 cm^{-1}).

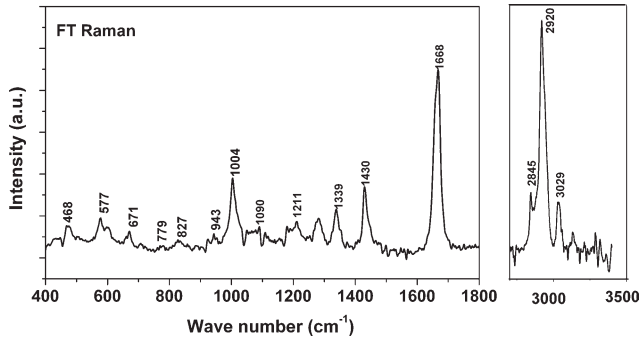

Figure 3 FT Raman spectrum of polychloroprene.

5 s and averaged over five accumulations. The spectral resolution obtained was about 3 cm^{-1}. The observed FT Raman spectra are shown in Figure 3.

THEORY

Calculation of normal mode frequencies

Normal mode calculation for an isolated polymeric chain was performed using Wilson's GF matrix method[18] as modified by Higg's[19] for an infinite polymeric chain. The vibrational secular equation to be solved is

$$|G(\delta)F(\delta) - \lambda(\delta)I| = 0 \; 0 \leq \delta \leq \pi \qquad (1)$$

where δ is the phase difference between the modes of adjacent chemical units, the $G(\delta)$ matrix is derived in terms of internal coordinates, with its inverse being the kinetic energy, and the $F(\delta)$ matrix is based on the Urey-Bradley force field.[16] The frequencies ν_i in cm^{-1} are related to eigen values by

$$\lambda_i(\delta) = 4\pi^2 c^2 \nu_i^2(\delta) \qquad (2)$$

A plot of ν_i (δ) versus δ gives the dispersion curve for the ith mode.

Calculation of heat capacity

Dispersion curves can be used to calculate the specific heat of a system. The density of state function is calculated from the relation

$$g(\nu) = \sum [(\delta\nu_j/\partial\delta)^{-1}]_{\nu j(\delta)=\nu j} \qquad (3)$$

The sum is over all the branches j. The constant volume heat capacity can be calculated using Debye's relation

$$C_v = \sum g(\nu_j) k N_A (h\nu_j/kT)^2 [\exp(h\nu_j/kT)/\{\exp(h\nu_j/kT) - 1\}^2] \qquad (4)$$

with $\int g(\nu_i)\, d\nu_i = 1$

RESULTS AND DISCUSSION

The crystal structure of trans 1,4-polychloroprene $(-C_\alpha H_2-CCl=CH-C_\beta H_2-)_n$ has been determined by Bunn[20] from X-ray diffraction results of oriented specimens. The unit cell is orthorhombic with space group P_{212121}. Each unit cell contains four molecules with a fiber repeat distance of 4.79 Å. The chlorine atom is displaced out of the plane of the —C—C=CH— group by 40° because of the repulsion between the bulky chlorine and nearby hydrogen atoms. There are 10 atoms in one repeat unit of TPCP which give rise to 26 optically active vibrations of non-zero frequencies. The four modes for which $\omega \to 0$ as $\delta \to 0$ are called acoustic modes. They are due to translation (one parallel and two perpendiculars to the chain axis) and one due to rotation around the chain axis.

The vibrational frequencies were calculated from the secular eq. (1) for values of δ varying from 0 to π in steps of 0.05 π. Initially approximate force constants were taken from the potential field data of β-trans 1,4-polyisoprene (β-TPI)[21] and those involving chlorine atoms from poly vinylidene chloride.[22] The initial force constants were transferred from polyisoprene because of its structural similarity with polychloroprene.[20] A replacement of CH_3 group by chlorine and *vice versa* will not significantly perturb the force field because of the group character of CH_3. Further the chlorine involving force constants were transferred from poly vinylidene chloride[22] because of the localized nature of modes related to chlorine atom. The accuracy was further judged by examining the effectiveness of force constants in other chlorine containing molecules e.g., poly vinyl chloride.[23] The set of force constants so composed was later refined to give the "best fit" to the observed spectra. We have used the Urey Bradley force field, which takes into account the bonded as well as nonbonded interactions. The assignments were made on the basis of potential energy distribution (PED), band shape, band intensity, and appearance/disappearance of modes in similar molecular groups placed in similar environment. The final force constants along with the internal coordinates are given in Table I. There is a wide difference in the force constants used by earlier workers[8,9] and the present one. This is much too obvious because the Urey Bradley force field covers a wide potential surface including nonbonded interactions and tension terms. This is widely reflected in the off-diagonal elements of F-matrix and the profile of the dispersion curves. These comments are relevant because Petcavich and Coleman[9] have used same force constants for both the systems polydichlorobutadiene and polychloroprene. That should not be done because the force constants are tied down with

TABLE I
Internal Coordinates and Urey Bradley Force Constants

Internal coordinates	Force constants	Internal coordinates	Force constants
$\nu[C_\alpha—H$	4.17	$\phi[C—C_\beta—H]$	0.56 (0.21)
$\nu[C_\alpha—C]$	4.40	$\phi[H—C_\beta—H]$	0.34 (0.295)
$\nu[C—Cl]$	2.5	$\phi[H—C_\beta—C_\alpha]$	0.30 (0.23)
$\nu[C=C]$	7.1	$\phi[C—C_\beta—C_\alpha]$	0.15 (0.18)
$\nu[C—H]$	4.75	$\phi[C_\beta—C_\alpha—H]$	0.28 (0.27)
$\nu[C—C_\beta]$	4.4	$\phi[C_\beta—C_\alpha—C]$	0.93 (0.50)
$\nu[C_\beta—H]$	4.24	$\phi[H—C_\alpha—H]$	0.36 (0.287)
$\nu[C_\beta—C_\alpha]$	3.8	$\phi[H—C_\alpha—C]$	0.58 (0.21)
$\phi[C_\alpha—C=C]$	0.74 (0.20)	$\omega[C—Cl]$	0.42
$\phi[C_\alpha—C—Cl]$	0.93 (0.55)	$\omega[C—H]$	0.20
$\phi[Cl—C=C]$	0.87 (0.20)	$\tau[C=C]$	0.045
$\phi[C=C—H]$	0.40 (0.20)	$\tau[C—C_\beta]$	0.010
$\phi[C=C—C_\beta]$	0.79 (0.50)	$\tau[C_\beta—C_\alpha]$	0.025
$\phi[H—C—C_\beta]$	0.43 (0.20)	$\tau[C_\alpha—C]$	0.060

ν, ϕ, ω, and τ denote stretch, angle bend, wagging, and torsion respectively.

Stretching force constants between the nonbonded atoms in each angular triplet (Gem configuration) are given in parentheses.

Unit of force constants for stretch is mdyne/A^0, for angle bend is mdyne Å rad^{-2} for wagging & torsion is mdyne A^0.

the structure. The matched frequencies along with their potential energy distribution (PED) are given in Tables II and III.

The dispersion curves are plotted in Figures 4(a) and 5(a) from 1000 to 1500 cm^{-1} and 0 to 1000 cm^{-1}, respectively. Since all the modes above 1500 cm^{-1} are nondispersive in nature, the dispersion curves are plotted only for the modes below 1500 cm^{-1}. For simplicity modes are discussed in two separate sections.

Nondispersive modes

In general, the nondispersive modes are the ones that are highly localized in nature. The free stretching modes generally fall in this region. e.g., C—H stretch, CH_2 symmetric and asymmetric stretches. The C—H stretching vibrations in the region from 2800 to 3100 cm^{-1} are highly localized and are in good agreement with the observed bands. Since the molecule contains two CH_2 groups, the absorption bands appear in pairs. They are slightly displaced from each other because of their placement in different environments and proximity to the chlorine atom. The C=C stretch frequency is calculated at 1654 cm^{-1} and is assigned to the peak at 1659 cm^{-1}. These frequencies occur in the region 1640–1670 cm^{-1} in several other polymeric systems also e.g., in trans 1,4-poly dichlorobutadiene,[24] poly dimethyl butadiene,[25] and trans 1,4 polyisoprene (α and β form).[21,26] These have been found to be the characteristic of a stable C=C bond (nonoxidative state) because the presence of any reactive species would have resulted in appearance/shift of a new absorption line. The C=C stretch frequency is used for the structural diagnosis of dienes. It has a higher value for trans configuration (1673 cm^{-1} in *trans*-1,4-polybutadiene[27]) as compared to *cis* configuration (1637 cm^{-1} in *cis*-poly 2-methyl 1,3 pentadiene[28]). The higher value in case of *trans* configuration is because of the lesser steric hindrances between atoms at 1 and 4 position making the double bond stress free.

Dispersive modes

The modes, which are nonlocalized in nature and are strongly coupled, electrically, mechanically or both, show appreciable dispersion e.g., torsion modes are strongly coupled with the neighboring unit and are dispersive. The actual dispersion of modes is discussed in the next section.

The scissoring modes of two CH_2 groups are calculated at 1443 and 1434 cm^{-1} and match well with the observed peaks at 1443 and 1431 cm^{-1} respectively, in IR. As commented earlier the difference between these two modes is due to the different environmental placement of two CH_2 groups. The modes reported by Wallen[11] at 1316, 1169, 1084, and 958 cm^{-1} and assigned to the crystalline part of the sample are observed at 1327, 1144, 1095, and 947 cm^{-1} respectively, in the second derivative FTIR spectra [Fig. 2(b)]. The constant difference of ± 10 wave numbers could easily be accounted for because of the scaling factor. The intensity of the corresponding modes is different because of the special treatment given by Wallen[11] to augment the intensity of crystalline and amorphous phases. The peak observed at 1327 cm^{-1} and attributed to the crystallinity has been assigned to the C—C stretch and bending vibrations of C=C—H and H—C—C_β. These conform to the assignments made by Tabb and Koenig.[8] All the bands related to the crystallinity are

TABLE II
Nondispersive Modes

	Obs.		
Calc.	IR	Raman	Assignment (% PED) at $\delta = 0$
3026	3024	3029	ν[C—H] (99)
2927	2918	–	$\nu[C_\beta—H]$ (95)
2908	2918	2920	$\nu[C_\alpha—H]$ (95)
2878	2883*	2862	$\nu[C_\beta—H]$ (96)
2861	2858	2845	$\nu[C_\alpha—H]$ (96)
1654	1660	1668	ν[C=C] (54), $\nu[C—C_\beta]$ (10)

All frequencies are in cm^{-1}.

Only dominant PED's are given.

* marked frequency is taken from second derivative FTIR spectra.

highly coupled normal modes and show a large dispersion. To make precise comments on the appearance/disappearance of absorption bands in a transition from amorphous to crystalline state, a full knowledge of crystalline structure is essential. It is well known that the vibrational spectra of a polymer chain, especially a semi crystalline polymer very much depend on the history of the polymer chain. The spectra are very much dictated by the amorphousity of the polymer and distribution and size of the amorphous regions. Reproducibility is very poor unless the past history of the polymer is wiped out by treatment such as annealing. This fact should be borne in mind in making assignments. The bands appearing in the region 1100–900 cm^{-1} are associated with C—C skeletal stretching modes.

The lower frequency modes (below 1000 cm^{-1}) need special mention, as there is difference in the assignments of these modes made by various authors.[8,9,17] The technique of inelastic neutron scattering[29] (INS) that is very useful in studying the low frequency vibrations in polymers has been applied to confirm the assignments of low frequency modes. Neutrons have high scattering cross section for protons (nearly 82 barns). Hence, one can monitor the normal modes through the motion of protons. Most of our assignments match with the observations of the INS reported by Kanaya et al.[17] Because of the symmetry dependent selection rules, only limited information regarding molecular dynamics can be obtained from infrared absorption and Raman scattering whereas neutron scattering being free from such constraints provides, at least in principle, full additional information about molecular systems. Also since the low-frequency vibrations are expected to depend sensitively on the chain conformation, neutron spectra are expected to provide some of these conformation sensitive modes more prominently, especially those which involve large amplitude of proton motion. e.g., the assignment of the band at 825 cm^{-1} in IR {ϕ [C_β-C_α-H] (21), ϕ [H-C_α-C] (15), ω[C-H] (12)} has been confirmed by inelastic neutron scattering measurements. Intensities in the neutron spectra are weighted by the vibrational amplitude of the motions of the hydrogen atoms. The peaks in the INS frequency distribution spectra can be identified with the regions of high density of states arising at the zone center or within the zone (reduced zone scheme).

The band observed at 825 cm^{-1} in IR has been assigned predominantly to C—H out of plane bending by Petcavich and Coleman[9] and to C—Cl stretching (20%) and Cl—C=C bending (14%) by Tabb and Koenig.[8] Mochel and Hall[30] have shown that this band cannot involve the C—Cl bond because it occurs within two wave numbers of the same place in the polybromoprene spectrum. According to them it should arise from a vibration consisting of a hydrogen deformation. Our calculations show that this mode consists mainly of angle bends of hydrogen ϕ[C_β-C_α-H], ϕ[H-C_α-C] and wagging of C—H with a small contribution from C—Cl stretching (12%). Kanaya et al.[17] have stated that in the inelastic neutron scattering, an intense and broad peak observed at 790 cm^{-1} should include the mode observed at 825 cm^{-1} in the IR spectrum and should not be due to the motion of chlorine atom. This gives further support to our assignment. This mode disperses and reaches at 861 cm^{-1} at $\delta = \pi$ where it is assigned to a new peak observed at 850 cm^{-1} in IR. It has major contribution from C—H out of plane bending at the zone boundary. In our calculations, C—Cl stretching is present in the modes calculated at 679 and 569 cm^{-1}. Mochel and Hall[30] have also identified the bands at 667 and 578 cm^{-1} in IR due to C—Cl stretching on comparison with the spectrum of polybromoprene. In inelastic neutron scattering,[17] no peaks are observed near these frequencies, which is suggestive of the fact that these modes are concerned with the motion of the chlorine atom. However, the PED of the mode calculated at 679 cm^{-1} contains C—H wagging also. On varying the force constant of ω [C—H] over a wide range (from 0.19 to 0.27 mdyne Å) this contribution does not disappear but on reaching the zone boundary the contribution of C—H wagging decreases and C—Cl stretching increases gradually.

The peak at 468 cm^{-1} in the Raman spectrum is attributed to C—Cl wagging. Kanaya et al.[17] have stated that in the inelastic neutron scattering, two weak peaks observed at 453 and 484 cm^{-1} correspond to this peak. One of these (453 cm^{-1}) is matched with the value calculated at the zone center (458 cm^{-1}) whereas the other one (484 cm^{-1}) is matched with the value calculated at the zone boundary (506 cm^{-1}). This assignment agrees with that of Petcavich and Coleman.[9] The C—C—Cl bending vibrations have been calculated at 407 and 321 cm^{-1}. The mode at 232 cm^{-1} is a torsional mode having contributions from various torsional motions τ [C_α—C], τ [C_β—C_α], and τ[C=C].

Characteristic features of the dispersion curves

Dispersion curves provide knowledge of the degree of coupling and information concerning the dependence of the frequency of a given mode on the sequence length of ordered conformations. In addition, the evaluation of dispersion curves for a three-dimensional (3D) system is somewhat involved both, in terms of dimensions and a large number of interactions. It is not easy to solve the problem without first solving it for a linear isolated chain. This alone can provide the best starting point. It has been

TABLE III
Normal Modes and Their Dispersion

Calc.	Obs. INS	Obs. IR	Obs. Raman	Assignment (%PED) ($\delta = 0$)	Calc	Obs. INS	Obs. IR	Obs. Raman	Assignment (%PED) ($\delta=\pi$)
1443	–	1443	–	ϕ [H-C_α-H] (44)+ ϕ [H-C_α-C] (33)+ν[C_α-C] (12)	1468	–	1443	–	ϕ [H-Cα-C] (23)+ ϕ [H-Cα-H] (17)+ν[Cα-C] (15)+ ϕ [C-C_β-H] (13)+ ν[C-C_β] (10)+ ν[C_β-Cα](9) ϕ [H-C_β-H] (6)
1434	–	1431	1430	ϕ [H-C_β-H] (36)+ ϕ [C-C_β-H] (33)+ν[C-C_β] (14)	1421	–	1431	1430	ϕ [H-C_β-H] (28)+ ϕ [H-Cα-H] (26)+ ϕ [C-C_β-H] (19) ϕ [H-Cα-C] (10))+ ν[C-C_β] (5)
1351	–	1346	1339	ϕ [H-C_β-H] (24)+ν[C_β-Cα](22)+ ϕ [H-C_α-H] (10) ϕ [H-C_β-Cα] (8)+ ϕ [C_β-Cα-H] (7)+ ν[C=C](5)	1363	–	1346	1339	ϕ [H-C_β-H] (27)+ν[C_β-Cα] (23)+ ϕ [H-Cα-H] (17)+ ϕ [C_β-Cα-H] (8)+ ϕ [H-C_β-Cα] (6)
1321	–	1327*	–	ϕ [C=C-H] (20)+ ϕ [H-C-C_β] (16)+ ϕ [C_β-C_α-H] (13) ν[C_β-Cα](11)+ ϕ [H-Cα-H] (10)+ ϕ [H-C_α-C] (10)	1322	–	1327*	–	ϕ [C=C-H] (18)+ ϕ [H-Cα-C] (14)+ ϕ [H-C-C_β] (9)+ ϕ [H-Cα-H] (8) ν[C_α-C] (8)+ ϕ [C_β-Cα-H] (6)+ ν[C=C](6)+ ν[C-Cl] (6)
1259	–	1261*	1253	ϕ [H-C_β-Cα] (20), ν[Cα-C] (18), ϕ [H-C_β-H] (11) ϕ [C-C_β-H] (10)+ ϕ [C_β-C_α-H] (9)+ ϕ [H-C_α-C] (8) ϕ [H-C_α-H] (7)	1242	–	1261*	1253	ϕ [H-C_β-Cα] (23), ϕ [C-C_β-H] (15), ϕ [H-C_β-H] (12) ϕ [H-C-C_β] (10)+ ϕ [C_β-C_α-H] (10)+ ϕ [C=C-H] (9)+ ϕ [H-C_α-C] (8)
1211	–	1205	1211	ϕ [C-C_β-H] (45), ϕ [H-Cα-C] (21)+ ϕ [H-C_β-C_α] (8) ϕ [C_β-Cα-H] (6)	1191	–	1205	1211	ϕ [C-C_β-H] (28)+ϕ [H-Cα-C] (19)+ϕ [C_β-Cα-H] (13) ϕ [H-C-C_β] (8)+ ν[Cα-C] (7)+ ϕ [H-C_β-C_α] (7)
1170	–	1144*	1180	ϕ [H-C_α-C] (29)+ν[Cα-C] (20)+ ϕ [H-C-C_β] (14) ϕ [C_β-C_α-H] (9)+ ϕ [C=C-H] (7)	1156	–	1144*	1180	ϕ [H-Cα-C] (46), ϕ [C-C_β-H] (20), ϕ [C_β-Cα-H] (18) ϕ [H-C_β-C_α] (6)
1115	–	1117	1110	ϕ [C-C_β-H] (25)+ϕ [H-Cα-C] (19)+ϕ [C_β-C_α-H] (15) ϕ [H-C_β-Cα] (15)+ν[Cα-C] (10)+ ν[C=C](5)	1127	–	1117	1110	ν[Cα-C] (33)+ϕ[C-C_β-H] (19)+ ϕ[H-C_β-Cα] (9)+ ϕ [H-C_β-Cα] (9)
1086	–	1095*	1090	ν[C-C_β] (49)+ϕ [C-C_β-H] (12)+ ϕ [H-C-C_β] (9)	1079	–	1095*	1090	ν[C-C_β] (45)+ϕ [C-C_β-H] (13)+ ϕ [H-C-C_β] (7)+ ϕ [C_β-Cα-C] (7)+ ν[C_β-C_α](7)+ ν[Cα-C] (5)
1009	–	999	1004	ν[C_β-C_α](42)+ϕ [C_β-Cα-H] (15)+ϕ [H-C_β-C_α] (14) ϕ [C_β-Cα-C] (6)+ϕ [C-C_β-H] (5)	1010	–	999	1004	ν[C_β-Cα](47)+ϕ [H-C_β-Cα] (14)+ϕ [C_β-Cα-H] (13)+ ϕ [C-C_β-H] (6)+ ϕ [C_β-Cα-C] (5)
951	–	947*	943	ϕ [C_β-Cα-H] (22)+ ω[C-H] (9)+ ω[C-Cl] (9) ϕ [Cl-C=C] (7)+ ϕ [H-C_β-Cα] (6)+ ν[C_β-Cα](5) τ[Cα-C] (5)+ ϕ [C_β-Cα-C] (5)+ ϕ [H-C_α-C] (5)	935	–	947*	943	ϕ [C_β-Cα-H] (39)+ϕ [H-C_β-Cα] (12)+ ϕ [H-C_α-C] (9)+ τ[Cα-C] (9)+ ϕ [Cα-C-Cl] (6)
834	790	825	827	ϕ [C_β-C_α-H] (21), ϕ [H-C_α-C] (15), ω[C-H] (12) ν[C-Cl] (12)+ ϕ [Cl-C=C] (10)+ ω[C-Cl] (7) τ[Cα-C] (6))+ϕ [C-C_β-H] (5)	861	790	850	827	ω[C-H] (29)+ω[C-Cl] (15)+ϕ [Cl-C=C] (13)+ ϕ [H-C_β-Cα] (11)+ ν[C-Cl] (9)
782	–	777	779	ϕ [H-C_β-Cα] (58)+ϕ [C-C_β-H] (11)+ τ[C_β-Cα](11)+ ϕ [C_β-C_α-H] (6)	771	–	777	779	ϕ [H-C_β-Cα] (45)+ϕ [C_β-Cα-H] (11)+τ[Cα-C] (11)+ τ[C_β-Cα](11)+ ϕ [C-C_β-H] (8)
679	–	658	671	ω[C-H] (51)+ ν[C-Cl] (22)+ τ[C=C] (9)+ ϕ [C_β-Cα-C] (5)	664	–	658	671	ω[C-H] (41)+ν[C-Cl] (27)+ τ[C=C] (9)

TABLE III. *Continued*

Calc.	Obs. INS	Obs. IR	Obs. Raman	Assignment (%PED) (δ = 0)	Calc	Obs. INS	Obs. IR	Obs. Raman	Assignment (%PED) (δ=π)
569	–	557*	577	ϕ [C=C-C_β] (23)+ν[C-Cl] (20)+ϕ [C_β-Cα-C] (16) ϕ [Cα-C-Cl] (13)+ τ[C_β-Cα](8)	514	–	557*	577	ν[C-Cl] (29)+ϕ[C_β-Cα-C] (21)+ ϕ[Cα-C-Cl] (9)+ ϕ [Cα-C=C] (7)+ ϕ [Cl-C=C] (7)+ ν[C=C](5) ω[C-Cl] (5)
458	453	471	468	ω[C-Cl] (33)+ϕ[Cα-C=C] (18)+ν[C-Cl] (11)+ ϕ [Cl-C=C] (8)	506	484	471	468	ϕ [C=C-C_β] (30)+ϕ [Cα-C=C] (15)+ν[Cα-C] (10)+ ϕ [Cα-C-Cl] (9)+ ν[C-C_β] (6)+ ϕ [Cl-C=C] (5)+ ϕ [H-C-C_β] (5)
407	–	418	–	ϕ [Cα-C-Cl] (45)+ ϕ [Cα-C=C] (14)+τ[Cα-C] (12) ν[C-Cl] (10)	438	–	418	–	ϕ [Cα-C-Cl] (26)+ν[C-Cl] (15)+ω[C-Cl] (12)+ ϕ [C_β-Cα-C] (8)+ ϕ [C-C_β-Cα] (5)
321	314	–	–	ϕ [C-C_β-Cα] (23)+ϕ [Cα-C=C] (19)+ϕ [Cl-C=C] (11) τ[C=C] (11)+ ϕ [C_β-Cα-C] (8)+ ϕ [H-C_β-Cα] (6)	334	314	–	–	ϕ [Cα-C-Cl] (18)+ϕ [C_β-Cα-C] (16)+τ[Cα-C] (12)+ τ[C=C] (9)+ ϕ [C-C_β-Cα] (9)+ ϕ [Cα-C=C] (9)+ ϕ [Cl-C=C] (8)
232	233	–	–	τ[Cα-C] (28)+τ[C_β-Cα](16)+τ[C=C] (14)+ ϕ [C_β-Cα-C] (12)+ ϕ [C=C-C_β] (6)	229	233	–	–	τ[Cα-C] (24)+ϕ [Cl-C=C] (12)+ϕ [C=C-C_β] (12)+ τ[C_β-Cα] (11)+ ϕ [Cα-C-Cl] (11)+ ϕ [Cα-C=C] (7)
162	175	–	–	τ[Cα-C] (17)+ϕ [Cα-C-Cl] (16)+ϕ [Cl-C=C] (15) ϕ [C_β-C_α-H] (9)+ τ[C=C] (7)+ ϕ [C=C-C_β] (7) τ[C_β-Cα](5)	172	175	–	–	ϕ [Cα-C=C] (20)+ϕ[C-C_β-Cα] (20)+ϕ[C_β-Cα-C] (18) ω[C-Cl] (9)

INS frequencies are from Ref. [17].
All frequencies are in cm^{-1}.
Only dominant PED's are given.
* are marked frequencies are taken from second derivative FTIR spectra.

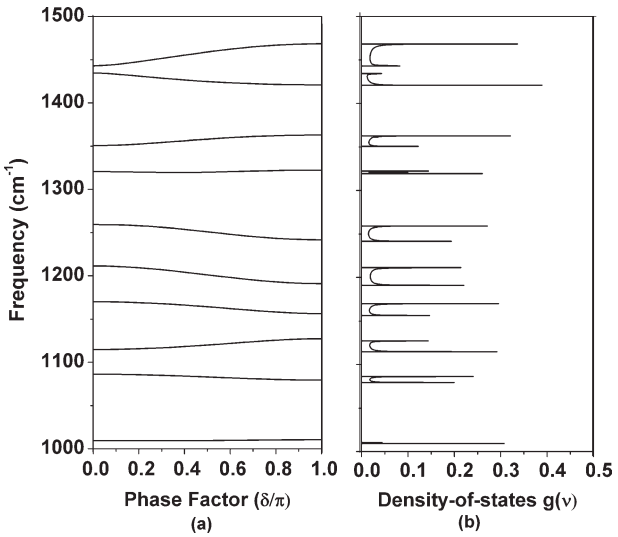

Figure 4 (a) Dispersion curves of polychloroprene (1000–1500 cm^{-1}). (b) Density-of-states of polychloroprene (1000–1500 cm^{-1}).

generally observed that, the intramolecular interactions (covalent and nonbonded) are generally stronger than the intermolecular interactions (hydrogen bonding and nonbonded). Crystal field only leads to splitting near the zone center and zone boundary. The basic profile of the dispersion curves remains more or less unaltered. Thus, the study of phonon dispersion in polymeric systems is an important study.

The two scissoring modes of CH_2 calculated at 1443 cm^{-1} and 1434 cm^{-1} at zone center diverge and reach 1468 cm^{-1} and 1421 cm^{-1} at the zone boundary. The mode at 1443 cm^{-1} consists mainly of ϕ[H—C_α—H] (44%) and ϕ[H—C_α—C] (33%). As δ increases, both these contributions decrease in this mode and start appearing in the lower mode that has contributions mainly from ϕ[H—C_β—H]. The presence of ϕ[H—C_α—H] in both the modes may be responsible for the divergence because of the repulsion in the energy momentum space from the zone center onto the zone boundary. The mode calculated at 1351 cm^{-1} disperses and reaches 1363 cm^{-1} at the zone boundary. As phase angle advances, the contribution of ϕ[H—C_β—H] increases in this mode and decreases in the higher frequency mode (1434 cm^{-1}) until it becomes almost same in both the modes.

The mode calculated at 407 cm^{-1} decreases gradually until $\delta = 0.5\ \pi$ where it shows region of high density of states and then it increases with increasing value of δ until zone boundary. The PED of this mode consists of ϕ[C_α—C—Cl] (45%), ϕ[C_α—C=C] (14%), τ[C_α—C] (12%), and ν[C—Cl] (10%). The percentage of ϕ[C_α—C—Cl], ϕ[C_α—C=C], and τ[C_α—C] decreases continually till the zone boundary. However, the contribution of stretch decreases till $\delta = 0.5\ \pi$ and then starts increasing. During its progression, it mixes with ϕ[Cl—C=C], ϕ[C_β—C_α—C], and ω[C—Cl] which may be responsible for the rise of dispersion curve.

The dispersion curves at 321, 232, and 162 cm^{-1} have flat regions around $\delta = 0.5\ \pi$ indicating high density of states. The presence of regions of high density of states also refers to some internal symmetry points in the energy momentum space and these are known as van Hove type singularities.[31] No crossing is present in the dispersion profile of the modes indicating the lack of the mirror plane of symmetry.[32]

The low-frequency vibrations are expected to depend sensitively on the chain conformation hence the dispersion curves of TPCP in the low-frequency region have been compared with those of β-

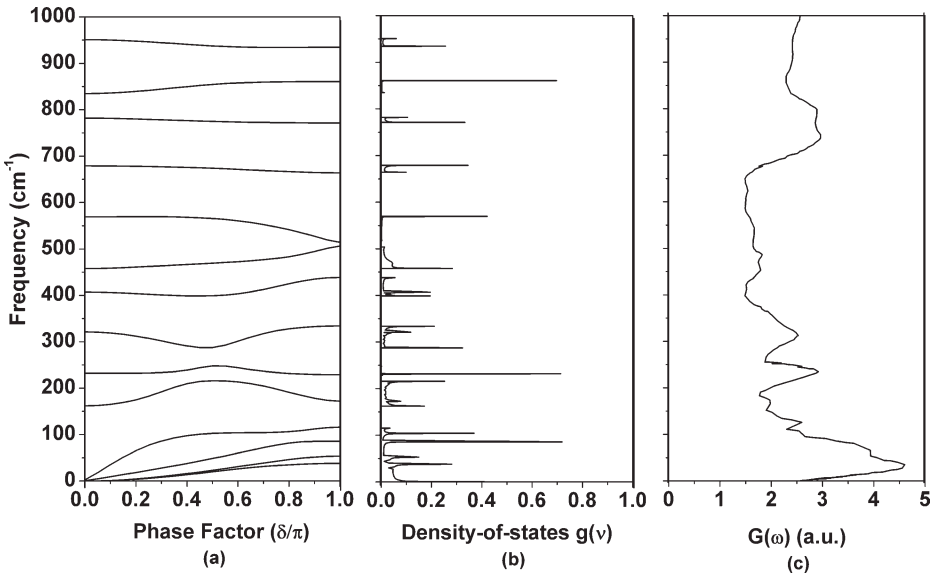

Figure 5 (a) Dispersion curves of polychloroprene below 1000 cm^{-1}. (b) Density of states curves of polychloroprene below 1000 cm^{-1}. (c) Inelastic neutron scattering of polychloroprene below 1000 cm^{-1} taken from reference.[17]

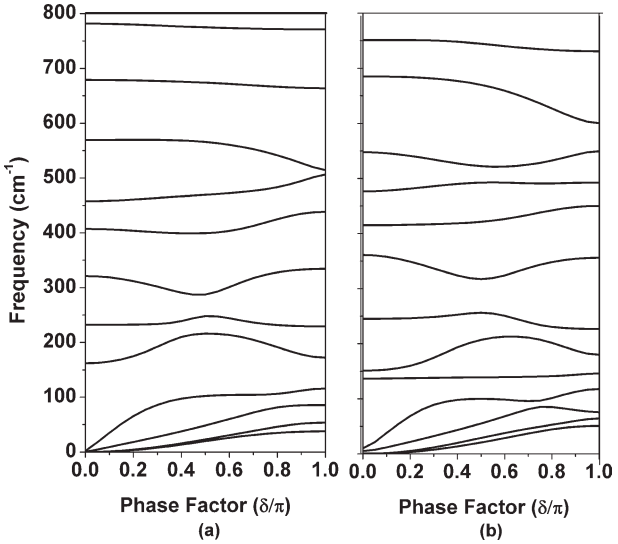

Figure 6 Comparison of low-frequency dispersion curves of (a) polychloroprene and (b) β-trans 1,4-polyisoprene.

polyisoprene $(CH_2C(CH_3)=CH-CH_2)_n$[21] (Fig. 6) which has conformation completely analogous to it.[20] A comparison of low-frequency modes in both the polymers shows that although the PED is not the same because of the presence of CH_3 group in β-polyisoprene[21] in place of chlorine atom but their dispersive behavior is similar. One of the characteristics of the dispersion curves is the similarity in profile and weak repulsion in the modes calculated at 232 and 162 cm^{-1}. These modes have contribution from torsions and skeletal angle bends. Although the mode at 162 cm^{-1} has contribution from chlorine angle bends also, these contributions decrease gradually and finally vanish at around $\delta = 0.5\ \pi$ and some other skeletal modes come in. In both these systems, the regions of high density of states are around the same value of phase factor (in the neighborhood of $\delta = 0.45\ \pi$ to $0.55\ \pi$). This is a common feature of the similar chain conformation and generally refers to internal symmetry. It is observed that the profiles of the acoustic modes in TPCP and β-TPI bear a great deal of resemblance.

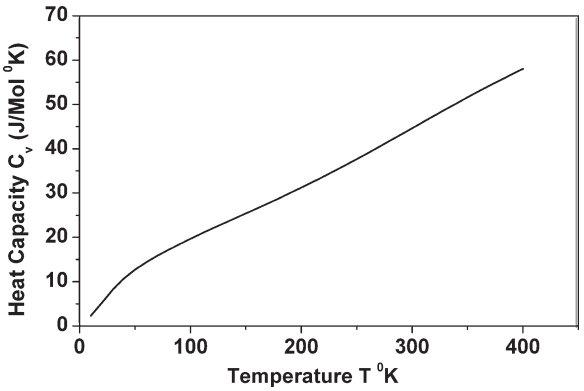

Figure 7 Variation of heat capacity C_v with temperature.

Frequency distribution function and heat capacity

From the dispersion curves, frequency distribution function has been obtained and plotted in Figures 4(b) and 5(b). The peaks in the frequency distribution curves correspond to the regions of high density of states (van Hove type singularities). For a one-dimensional system, the density of state function or the frequency distribution function expresses the way energy is distributed among the various branches of normal modes in the crystal. On considering a solid as an assembly of harmonic oscillators, the frequency distribution $g(\nu)$ is equivalent to a partition function. The knowledge of density of states can be used to obtain the thermodynamic properties such as heat capacity, enthalpy, etc. We have calculated the heat capacity of TPCP in the temperature range of 10–400 K using Debye's equation. This is plotted in Figure 7. The heat capacity follows the usual curve that is linear at low temperatures and tends towards nonlinearity at higher temperatures (classical region). Although the heat capacity is predictive in nature but it may stimulate some worker to carry out measurements at a later date.

CONCLUSIONS

The Wilson's GF matrix method as modified by Higg's along with the Urey Bradley force field has successfully explained the spectroscopic data on TPCP. Several unassigned modes have been assigned and predictive values of heat capacity as a function of temperature within the range 10–400K have been given. However, the contribution from the lattice modes is bound to make a difference to the specific heat because of its sensitivity to these modes. Despite several limitations involved in the calculation of specific heat and absence of experimental data, this study would provide a good starting point for further basic studies on thermodynamical behavior of polymers.

Financial support to one of the authors (PT) from the Alexander von Humboldt Foundation, Germany and the Department of Science and Technology, New Delhi under Indo-Russian project is gratefully acknowledged. We are thankful to Prof. H.W. Siesler and Prof. Arnulf Materny for their kind help in obtaining FTIR and Raman spectra.

References

1. Keibal, N. A.; Bondarenko, S. N.; Kablov, V. F.; Goryainov, I. Y. Polym Sci Series D Glues Sealing Mater 2008, 1, 151.
2. Rajalingam, P.; Radhakrishnan, G. Polym Int 1990, 25, 87.
3. Budrugeac, P.; Segal, E. J Thermal Analysis Calorimetry 1998, 53, 441.
4. Ha-Anh, T.; Vu-Khanh, T. Polym Test 2005, 24, 775.
5. Maynard, J. T.; Mochel, W. E. J Polym Sci 1954, 13, 235.
6. Maynard, J. T.; Mochel, W. E. J Polym Sci 1954, 13, 251.

7. Tabb, D. L.; Koenig, J. L.; Coleman, M. M. J Polym Sci Phys Ed 1975, 13, 1145.
8. Tabb, D. L.; Koenig, J. L. J Polym Sci Phys Ed 1975, 13, 1159.
9. Petcavich, R. J.; Coleman, M. M. J Macromol Sci Phys B 1980, 18, 47.
10. Arjunan, V.; Subramanian, S.; Mohan, S. Turk J Chem 2003, 27, 423.
11. Wallen, P. J. Spectrochim Acta A 1991, 47, 1321.
12. Chaturvedi, D.; Mishra, S.; Tandon, P.; Gupta, V. D.; Siesler, H. W. J Polym Eng Sci 2009, 49, 850.
13. Jain, A.; Mishra, R. M.; Tandon, P.; Gupta, V. D. J Macromol Sci 2006, 45, 263.
14. Kumar, N.; Shukla, S. K.; Tandon, P.; Gupta, V. D. J Polym Sci Part B: Polym Phys 2009, 47, 2353.
15. Mishra, R. M.; Jain, A.; Tandon, P.; Wartewig, S.; Gupta, V. D. Chem Phys Lipids 2006, 142, 70.
16. Urey, H. C.; Bradley, C. A. Phys Rev 1931, 38, 1969.
17. Kanaya, T.; Ohkura, M.; Kaji, K. Bull Inst Chem Res, Kyoto Univ 1989, 67, 68.
18. Wilson, E. B.; Decius, J. C.; Cross, P. C. Molecular Vibrations: The Theory of Infrared and Raman Vibrational Spectra; Dover Publications: New York, 1980.
19. Higg's, P. W. Proc Roy Soc (London) 1953, A220, 472.
20. Bunn, C. W. Proc Royal Soc London Ser A 1942, 180, 40.
21. Pathak, A.; Saxena, V.; Tandon, P.; Gupta, V. D. Polymer 2006, 47, 5154.
22. Gopal, S. A Study of Ionic Conduction and Phonon Dispersion in Some Polymeric Systems. Ph.D. Thesis, University of Lucknow, Lucknow, India, 1996.
23. Tasumi, M.; Shimanouchi, T. Polymer J 1971, 2, 62.
24. Gupta, A.; Choudhary, N.; Bee, S.; Tandon, P.; Gupta, V. D. Polym Sci Ser A 2010, 52, 1057.
25. Petcavich, R. J.; Coleman, M. M. J Polym Sci: Polym Phys Ed 1980, 18, 2097.
26. Pathak, A.; Agarwal, R.; Tandon, P.; Gupta, V. D. J Macromol Sci Part B: Phys 2007, 46, 245.
27. Rastogi, S.; Tandon, P.; Gupta, V. D. J Macromol Sci Phys B 1998, 37, 683.
28. Misra, N. K.; Kapoor, D.; Tandon, P.; Gupta, V. D. J Macromol Sci Phys 2000, 39, 39.
29. Gupta, V. D.; Trevino, S.; Boutin, H. J Chem Phys 1968, 48, 3008.
30. Mochel, W. E.; Hall, M. B. J Am Chem Soc 1949, 71, 4082.
31. Callaway, J. Quantum Theory of Solids; Academic Press: New York, 1974; p 30.
32. Bower, D. I.; Maddams, W. F. The Vibrational Spectroscopy of Polymers; Cambridge University Press: Cambridge, 1989.